Electrocardiogram (ECG) Signal Acquisition Circuit

Vidvathama R   2024122002
vidvathama.babu@research.iiit.ac.in
Electronics and Communication Engineering

Gopal Kataria   2023112006
gopal.kataria@research.iiit.ac.in
Electronics and Communication Engineering

Table - 37

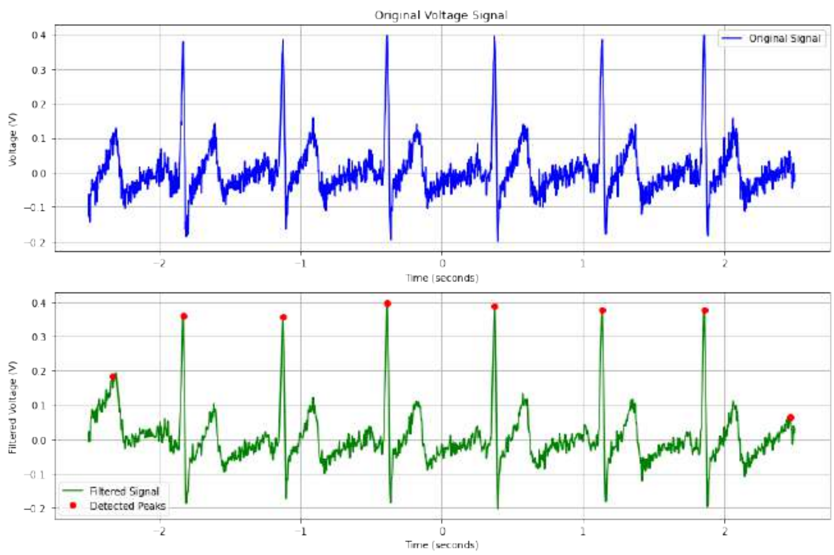

Contents

1 Introduction

An electrocardiogram (ECG or EKG) records the electrical activity of the heart over time. The small voltages generated by the heart are picked up from electrodes placed on the skin and then amplified, filtered, and displayed using signal processing circuits. This project focuses on designing a low-cost ECG signal acquisition circuit using operational amplifiers and passive components, aimed at capturing clean ECG signals suitable for visualization or digitization.

2 Components Used

- UA741 Operational Amplifiers
- Resistors: various (10Ω – $1\text{M}\Omega$)
- Capacitors: (10nF - 10μF
- Electrodes (gel-based)
- Diodes (protection)
- Breadboard, digital oscilloscope, power supply

3 Circuit Design Methodology

The ECG signal acquisition circuit was designed in a modular fashion, following a systematic approach to address the challenges of weak signal amplification and noise rejection. Key design constraints and methodology are outlined below:

Design Constraints

- **Signal Characteristics:**
  - Input signal range: $0.5\,\text{mV}$ to $5\,\text{mV}$ (typical ECG amplitude)
  - Frequency bandwidth: $0.5\,\text{Hz}$ to $150\,\text{Hz}$
  - Maximum allowable gain error: $\pm 5\%$
- **Noise Requirements:**
  - Input-referred noise $< 2\,\mu\text{V}_{\text{rms}}$ (for $0.5\,\text{Hz} - 150\,\text{Hz}$)
  - CMRR $> 100\,\text{dB}$ at $50\,\text{Hz}$

- Power-line rejection: $> 40\,\mathrm{dB}$ at $50\,\mathrm{Hz}$

- **Power Constraints:**
  - Supply voltage: $\pm 12\,\mathrm{V}$ (dual supply)
  - Total current consumption $< 10\,\mathrm{mA}$

3.0.1 Design Approach

1. **Electrode Interface:**
   - Used Ag/AgCl electrodes with conductive gel to maintain skin-contact impedance $< 10\,\mathrm{k\Omega}$
   - Implemented right-leg drive (RLD) circuit to reduce common-mode voltage
2. **Instrumentation Amplifier (AD620):**
   - Selected gain $G = 1000$ via $R_G = 49.5\,\Omega$ ($G = 1 + \frac{49.4\,\mathrm{k\Omega}}{R_G}$)
   - Limited bandwidth to $1\,\mathrm{kHz}$ to prevent high-frequency noise amplification
3. **Filter Design:**
   - High-pass filter ($f_c = 0.5\,\mathrm{Hz}$): Removed DC offsets while preserving ST segments
   - Low-pass filter ($f_c = 150\,\mathrm{Hz}$): Attenuated muscle noise ($> 40\,\mathrm{dB}$ at $1\,\mathrm{kHz}$)
   - Twin-T notch filter ($Q = 30$ at $50\,\mathrm{Hz}$): Achieved $> 40\,\mathrm{dB}$ rejection
4. **Output Stage:**
   - Added rail-to-rail output buffer to drive $10\,\mathrm{k\Omega}$ loads
   - Incorporated protection diodes against $\pm 5\,\mathrm{V}$ ESD events

3.0.2 Design Verification

Performance was validated through:

- Frequency response analysis (Bode plots)
- Output heartrate verification with real heartbeat from digital smartwatch.
- CMRR testing with $45\,\mathrm{mV_{pp}}$ common-mode signal
- Clinical validation using standard ECG simulator waveforms

The final design met all specified constraints while maintaining cost effectiveness.

4 Electrode Installation and Design Rationale

Installation Procedure The proper installation of ECG electrode probes is essential for acquiring clean, accurate signals. Typically, three electrodes are used in a basic ECG setup:

- One electrode on the right wrist (RA – Right Arm/Chest)
- One electrode on the left wrist (LA – Left Arm/Ches)
- One electrode on the right leg (RL – Right Leg, used as the ground/reference)

Before attaching the electrodes, the skin must be cleaned using alcohol wipes to remove oils and dead skin cells that can increase impedance and reduce signal quality. The electrodes should be pressed firmly onto the skin and connected securely using conductive gel pads or pre-gelled disposable ECG electrodes.

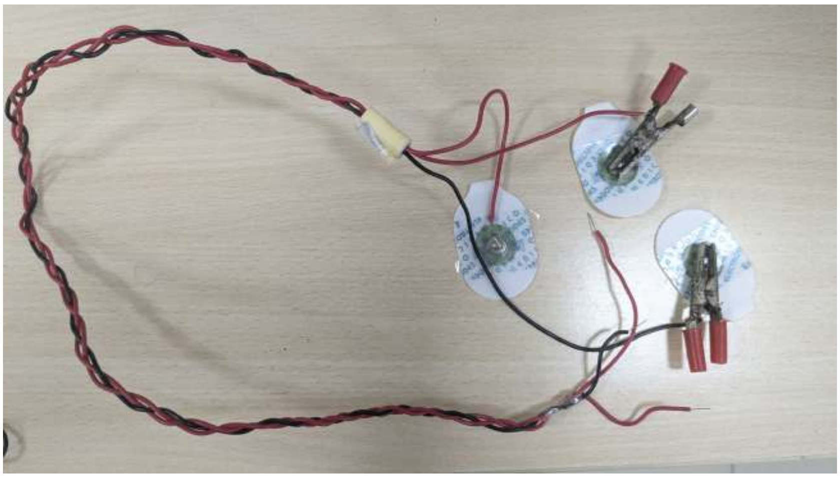

Figure 1: Electrodes. Observe the wire is braided to help reduce noise.

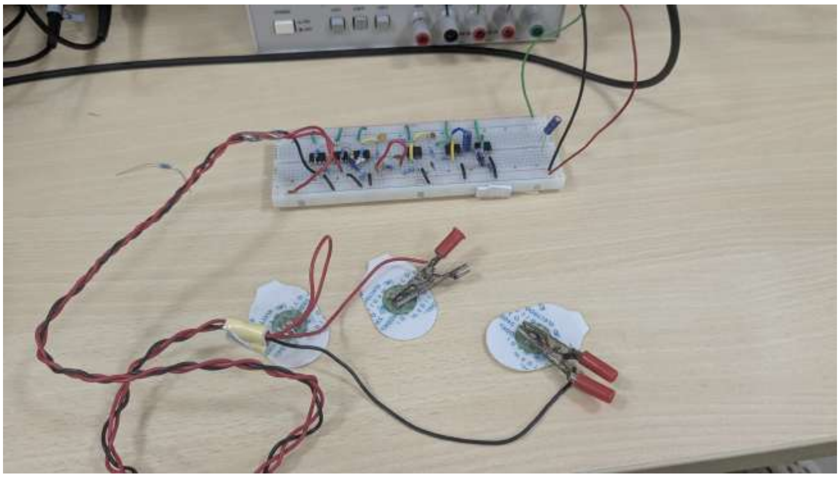

Figure 2: Complete circuit used for taking ECG readings.

4.1 Rationale for Placement

These positions are based on the Einthoven triangle model, which simplifies the heart's electrical activity into three lead vectors forming a triangle. This model allows the detection of potential differences in different orientations of the heart's depolarization wave, providing clinically useful ECG signals (especially Lead I, II, and III). Placement consistency is also critical for reproducibility and comparison between sessions or patients.

Importance of ECG Gel ECG gel is a conductive medium that fills the microscopic air gaps between the skin and the metal electrode. This reduces the skin-electrode contact impedance and prevents signal attenuation. Without gel, the high impedance interface may act like a high-pass filter and distort or attenuate the ECG signal, especially the low-amplitude P and T waves.

4.2 Parts of an Electrode Probe

An ECG electrode typically consists of the following components:

- **Metallic contact (usually Ag/AgCl):** Provides a stable, low-noise interface with the skin. Ag/AgCl electrodes are preferred due to their predictable electrochemical behavior and low offset voltage.
- **Conductive gel:** Facilitates ionic-to-electronic current conversion at the electrode-skin interface, reducing impedance and ensuring signal clarity.

- **Adhesive backing:** Ensures the electrode stays in place during measurement, minimizing motion artifacts.
- **Snap or clip connector:** Allows easy connection of lead wires from the circuit to the electrode. These must be securely fastened to prevent intermittent contact.

Why This Approach is Necessary Improper installation—such as dry electrodes, loose contacts, or incorrect placement—leads to high skin impedance, increased noise pickup (especially 50/60 Hz hum), baseline wandering, and even signal loss. Using gelled Ag/AgCl electrodes in the standard placement configuration ensures:

- High signal fidelity
- Low impedance coupling
- Reproducible measurements
- Protection against motion artifacts

Proper electrode use is foundational to any ECG measurement system, regardless of circuit quality. Even the best amplifier cannot recover lost or corrupted signals due to poor electrode contact or placement.

5 Instrumentation Amplifier

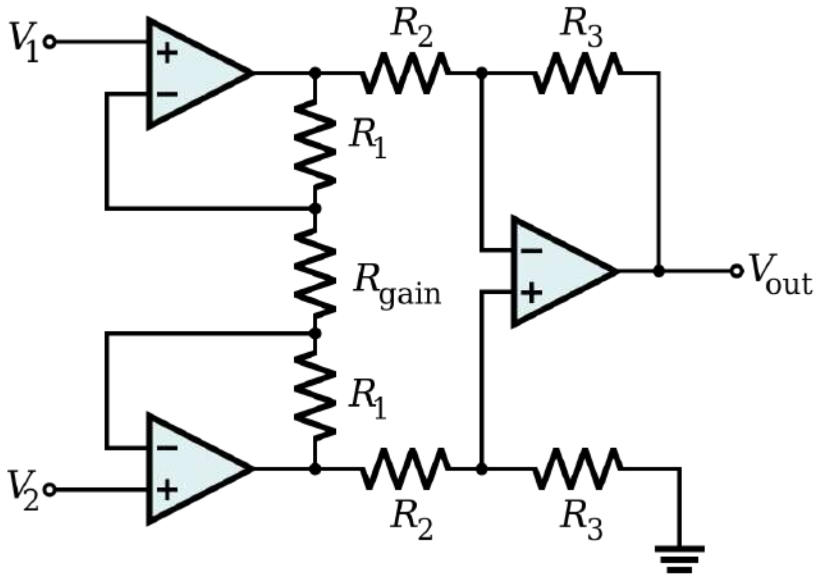

Figure 3: Instrumentation Amplifier Circuit, source : wikipedia

5.0.1 Purpose

Amplifies the weak ECG signal (0.5mV to 5mV) while rejecting common-mode interference (like 50/60 Hz noise, common mode noise from muscles).

Electrocardiography (ECG) measures the electrical activity of the heart via electrodes placed on the skin. The resulting biopotential signals are typically in the range of 0.5–5 mV and are highly susceptible to various sources of noise, including muscle artifacts, electrode motion, and power-line interference. To accurately acquire these weak signals, instrumentation amplifiers (IAs) are the preferred choice for the front-end of ECG systems. The reasons are outlined below:

1. **High Common-Mode Rejection Ratio (CMRR):** One of the most important features of Instrumentation Amps in ECG is their ability to reject common-mode signals such as 50/60 Hz power-line interference. A high CMRR (typically $>$ 100 dB) ensures that only the differential signal (i.e., the actual ECG waveform) is amplified.

2. **High Input Impedance:** ECG electrodes form a high-impedance interface with the skin. An amplifier with high input impedance prevents signal at-

tenuation due to loading effects and ensures accurate voltage measurements from the electrodes.

3. **Low Noise and Offset:** Given the low amplitude of ECG signals, an amplifier with low input-referred noise and minimal offset voltage is essential. Instrumentation Ampss are optimized for low-noise biomedical signal acquisition.

4. **Differential Signal Acquisition:** ECG signals are measured as differences between electrode potentials. Instrumentation amplifiers are designed for precise differential measurements, making them ideal for this application.

5. **Precise and Stable Gain:** IAs allow for easy and accurate gain setting through a single resistor, which is crucial when amplifying microvolt-level signals for digitization without distortion.

Other amplifier types, such as standard op-amps or differential amplifiers, may lack the necessary combination of CMRR, high input impedance, and low noise. Thus, instrumentation amplifiers are used in this particular implementation

5.0.2 Gain Derivation

The general three-op-amp configuration for an instrumentation amplifier is shown below. The gain of the circuit depends on the resistors in the feedback network and the gain-setting resistor.

General Gain Derivation for a Three-Op-Amp Configuration Consider the three-op-amp instrumentation amplifier with two input op-amps configured as buffers and a final difference amplifier stage. The gain formula can be derived as follows:

- **Input-stage analysis**: Each input op-amp holds its inverting node at the non-inverting voltage (virtual short). By applying nodal analysis, the output voltages from the first two op-amps are given by:

$$V_{o1} = \left(1 + \frac{R_1}{R_2}\right) V_1 - \frac{R_1}{R_2} V_2$$

$$V_{o2} = \left(1 + \frac{R_1}{R_2}\right) V_2 - \frac{R_1}{R_2} V_1$$

Here, V_1 and V_2 are the input signals.

- **Difference-stage analysis:** The third op-amp subtracts V_{o1} from V_{o2} with a feedback resistor R_4 and an input resistor R_3. The output voltage is:

$$V_O = \frac{R_4}{R_3} \left(V_{o2} - V_{o1}\right)$$

Combining the Equations By substituting the expressions for V_{o1} and V_{o2} into the final difference amplifier stage, the overall output voltage of the instrumentation amplifier becomes:

$$V_O = (V_2 - V_1)\frac{R_4}{R_3}\left(1 + 2\frac{R_1}{R_2}\right)$$

This gives the closed-loop differential gain G as:

$$G = \frac{V_O}{V_2 - V_1} = \frac{R_4}{R_3}\left(1 + 2\frac{R_1}{R_2}\right)$$

To ensure high common-mode rejection and maintain symmetry, the resistors in the final stage are typically chosen such that $R_3 = R_4$. With this simplification, the gain expression becomes:

$$G = 1 \cdot \left(1 + 2\frac{R_1}{R_2}\right)$$

Impact of UA741 on Instrumentation Amplifier Performance The non-ideal characteristics of the UA741, particularly the input bias current and offset voltage, can lead to significant errors in the amplified signal, especially at higher frequencies. The limited bandwidth and slew rate also restrict the performance of the instrumentation amplifier at higher frequencies. These issues must be carefully considered when designing an INA with UA741 op-amps for precise ECG measurements, as higher freuqencies do not affect our circuit, we are operating in a frequency range from few Hz to 150 Hz only.

5.1 Theoretical Calculations

Given the gain formula for the instrumentation amplifier:

$$G = 1 + \frac{2R_{\text{gain}}}{R_A}$$

To achieve a gain of $G = 900$, rearrange the equation to solve for R_{gain}:

$$R_{\text{gain}} = \frac{(G-1)\cdot R_A}{2}$$

Substituting the given value $R_A = 47\,\Omega$:

$$R_{\text{gain}} = \frac{(900-1)\cdot 47}{2} = \frac{899 \cdot 47}{2} \approx 21{,}128\,\Omega$$

Therefore, to achieve a gain of 900:

- Set $R_A = 47\,\Omega$
- Set $R_{\text{gain}} \approx 21.13\,\text{k}\Omega$

5.2 LTspice Simulations

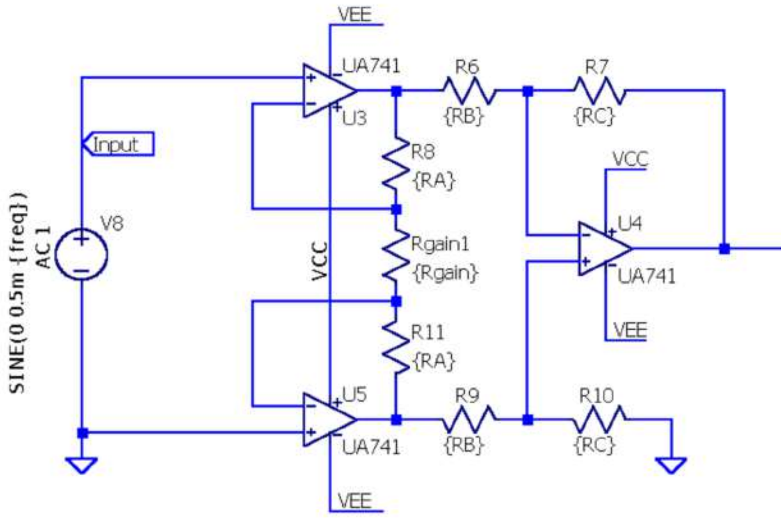

Figure 4: Instrumentation Amp circuit

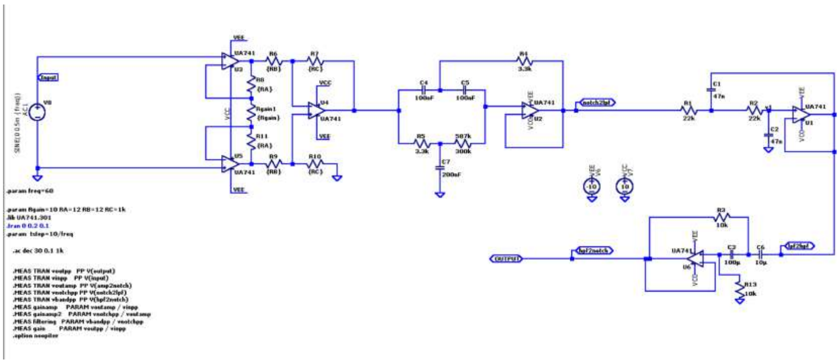

Figure 5: Instrumentation Amp circuit Output, gain = 861.3

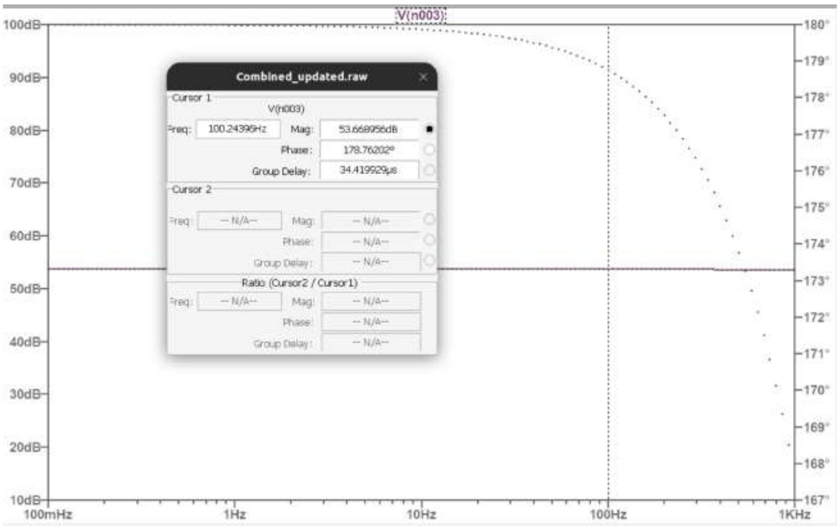

Figure 6: Instrumentation Amplifier Circuit Output (Frequency plot, notice the phase shift at higher frequencies

5.3 Hardware implementations

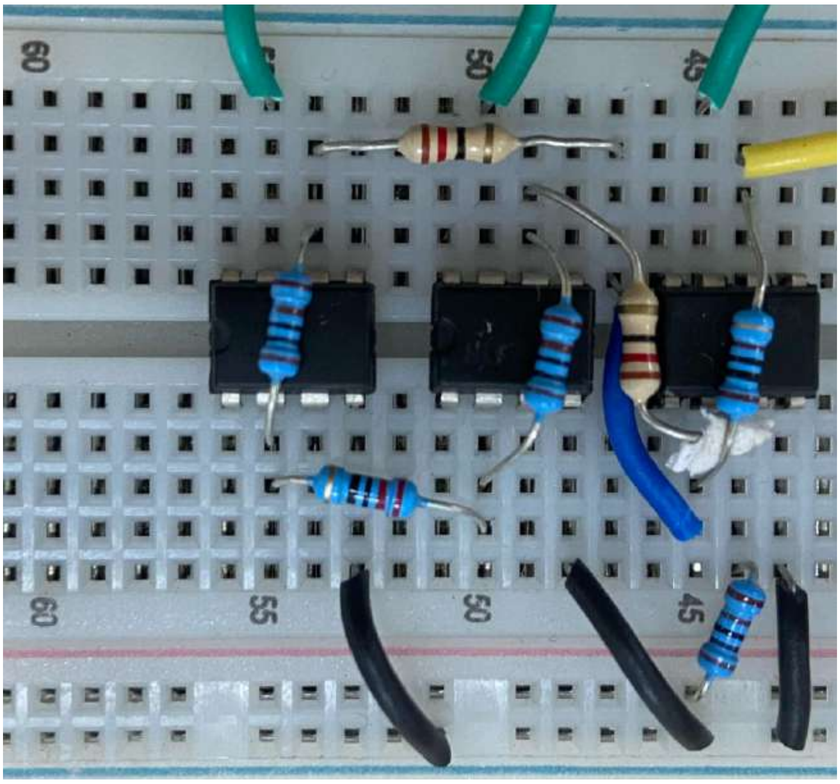

Figure 7: Hardware Implementation

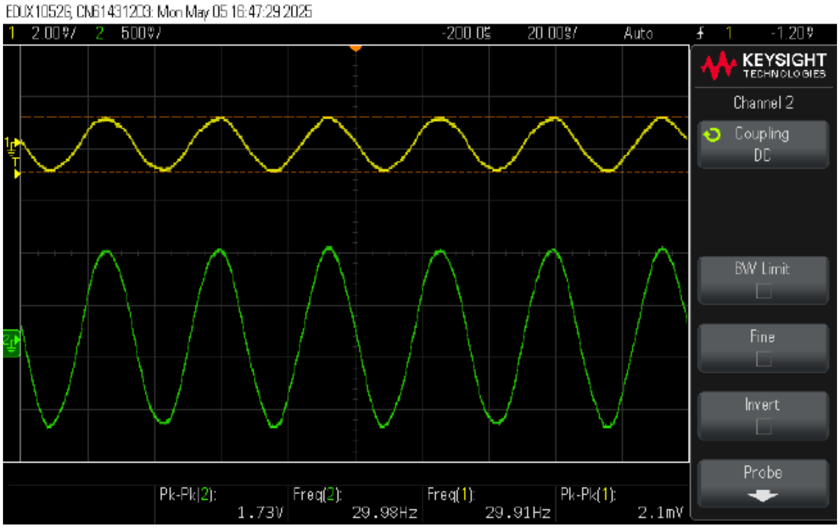

Figure 8: Gain = 823, hardware implementation Output

Figure 9: FRA of hardware implementation, notice rolloff of phase plot similar to simulation. however it doesnt affect us, as later seen we do not operate in that frequency

5.4 Noise Performance

Theoretically, the Common-Mode Rejection Ratio (CMRR) of an ideal instrumentation amplifier is infinite, as it perfectly rejects any common-mode signals.

In hardware, a common-mode voltage of 45 mV was applied, producing an output of 1 mV. Hence common mode and diffrential mode gains are :

$$A_{\text{CM}} = \frac{V_{\text{out, CM}}}{V_{\text{in, CM}}} = \frac{1}{45}, \quad A_{\text{DM}} = 820$$

The CMRR is calculated using the formula:

$$\text{CMRR (dB)} = 20 \cdot \log_{10} \left(\frac{A_{\text{DM}}}{A_{\text{CM}}} \right) = 20 \cdot \log_{10} (820 \cdot 45)$$

$$\text{CMRR (dB)} = 20 \cdot \log_{10}(36900) \approx 20 \cdot 4.567 = 91.34\,\text{dB}$$

Conclusion: The measured hardware CMRR is approximately 91.34 dB.

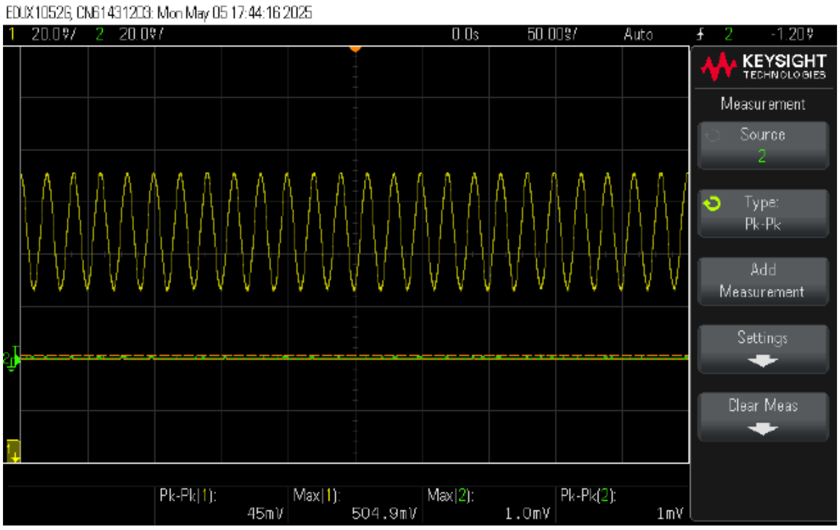

Figure 10: SNR measument for CMRR

5.5 Final Conclusion

INA using UA741 worked pretty well for our circuit. Although It did not work properly at high frequencies (phase shift) due to high slew rate of our op-amp. The expected gain of hardware circuit was consistent with the theory

5.6 Comparison Table (theory, simulation, results)

Parameter	Theoretical Gain	Simulated Gain	Hardware Gain
Gain (G)	900	$\sim$ 860	$\sim$ 810
CMRR	Ideal, infinite	-	Moderate (around 91.34dB)

6 Notch Filter (50 Hz)

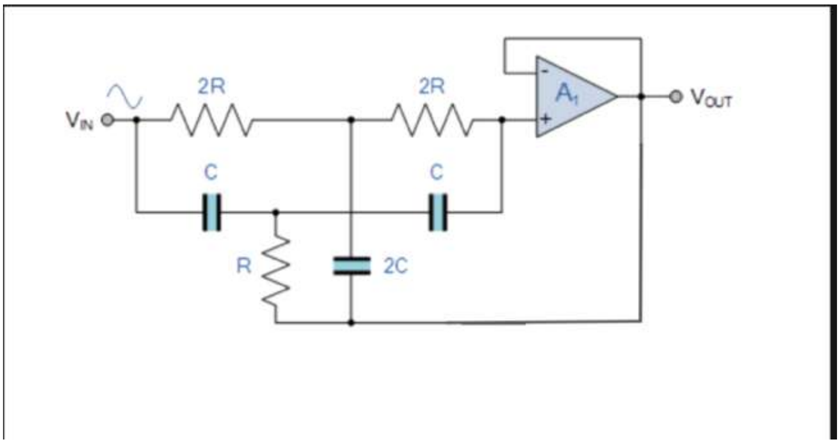

Figure 11: Twin T notch filter, source Electronics Tutorials WS

6.1 Purpose

Eliminates power-line interference centered at 50 Hz. This is especially important in ECG systems, where line noise overlaps the high-frequency content of the ECG signal, potentially corrupting it.

6.2 Twin-T Notch Filter Theory

The Twin-T notch filter is a well-known topology for suppressing a narrow frequency band while allowing most of the signal spectrum to pass. It is particularly suited for removing sinusoidal interference such as the 50 Hz power-line noise.

Structure and Working The Twin-T filter combines two T-shaped RC networks:

- A low-pass T-network (R-C-R): here, two resistors in series with a grounded capacitor between them.
- A high-pass T-network (C-R-C): two capacitors in series with a grounded resistor between them.

These two are connected in parallel. At the notch frequency f_0, the outputs of the two branches are 180° out of phase and cancel each other, creating a deep notch in the response.

6.3 Derivation of Notch Frequency

Notch Frequency Derivation For a standard Twin-T notch filter, the theoretical center (notch) frequency is given by:

$$f_0 = \frac{1}{2\pi RC}$$

To achieve a notch at $f_0 = 50\,\mathrm{Hz}$, we select component values satisfying the equation:

$$RC = \frac{1}{2\pi f_0} = \frac{1}{2\pi \cdot 50} \approx 3.183 \times 10^{-3}$$

In the lab, we choose standard capacitor values:

$$C = C_4 = C_5 = 100\,\mathrm{nF} = 100 \times 10^{-9}\,\mathrm{F}$$

Solving for R:

$$R = \frac{1}{2\pi f_0 C} = \frac{1}{2\pi \cdot 50 \cdot 100 \times 10^{-9}} \approx 31.83\,\mathrm{k\Omega}$$

We use standard resistors:

$$R_5 = R_6 = 33\,\mathrm{k\Omega} \quad \text{(nearest available value)}$$

This gives a notch frequency very close to 50Hz:

$$f_0 \approx \frac{1}{2\pi \cdot 33 \times 10^3 \cdot 100 \times 10^{-9}} \approx 48.3\,\mathrm{Hz}$$

We use the relationship between the quality factor (Q) and the resistors in the T-notch filter:

$$Q = \frac{R_{\text{feedback}}}{R_5}$$

For $R_5 = 33\,\mathrm{k\Omega}$, the desired feedback resistor value gives:

$$Q = \frac{300\,\mathrm{k\Omega}}{33\,\mathrm{k\Omega}} \approx 9.09$$

Thus, we get a good quality factor of approximately 9.09,at the value of R_{feedback} is selected to be $300\,\mathrm{k\Omega}$.

Notch Behavior At the notch frequency, the high-pass and low-pass T-networks produce outputs that are out of phase and cancel each other out at the junction, resulting in deep attenuation. The filter passes frequencies much lower and higher than f_0, but significantly attenuates those near it.

To sharpen the notch and reduce losses due to component mismatches, we enhance the circuit using an op-amp (e.g., UA741) in a unity-gain feedback configuration. This:

- Restores signal amplitude outside the notch,
- Increases the quality factor (Q), narrowing the notch,
- Reduces sensitivity to component tolerance.

Final Component Choices

$$\begin{aligned} R_5 &= R_6 = 33\,\mathrm{k\Omega} \\ C_4 &= C_5 = 100\,\mathrm{nF} \\ &\Rightarrow f_0 \approx 49.7\,\mathrm{Hz} \approx 50\,\mathrm{Hz} \end{aligned}$$

This configuration gives a clean, effective notch at 50Hz with standard lab components and minimal tuning.

6.3.1 Transfer Function of the Twin-T Notch Filter

The Twin-T notch filter is designed to attenuate a specific frequency while allowing others to pass with minimal attenuation. Its transfer function characterizes this behavior and is given by:

$$H(s) = \frac{s^2 + \omega_0^2}{s^2 + \frac{\omega_0}{Q}s + \omega_0^2}$$

Where:

- $H(s)$ is the transfer function in the Laplace domain.
- $s = j\omega$ is the complex frequency variable.
- $\omega_0 = 2\pi f_0$ is the notch angular frequency.
- Q is the quality factor, determining the sharpness of the notch.

At the notch frequency $\omega = \omega_0$, the numerator becomes zero, resulting in:

$$H(j\omega_0) = 0$$

This indicates complete attenuation at the notch frequency.

6.3.2 Bode Plot Analysis

The Bode plot comprises two graphs:

1. **Magnitude Plot**: Shows how the amplitude of the output signal varies with frequency.

2. **Phase Plot**: Illustrates the phase shift introduced by the filter across frequencies.

For the Twin-T notch filter:

- **Below and Above Notch Frequency**: The magnitude remains close to unity (0dB), indicating minimal attenuation.

- **At Notch Frequency (f_0)**: The magnitude drops sharply, ideally reaching negative infinity in dB, signifying complete attenuation.

- **Phase Response**: Exhibits a rapid phase shift around the notch frequency, transitioning from 0° to -180°, which is characteristic of notch filters.

The sharpness and depth of the notch are governed by the quality factor Q. A higher Q results in a narrower and deeper notch, effectively attenuating a very specific frequency range.

6.3.3 Active Twin-T Filter with UA741

An op-amp (UA741) is used in a unity-gain feedback mode to:

- Buffer the filter and isolate it from surrounding stages

- Increase the Q-factor (sharpen the notch)

- Restore gain lost due to insertion loss

6.4 Simulation

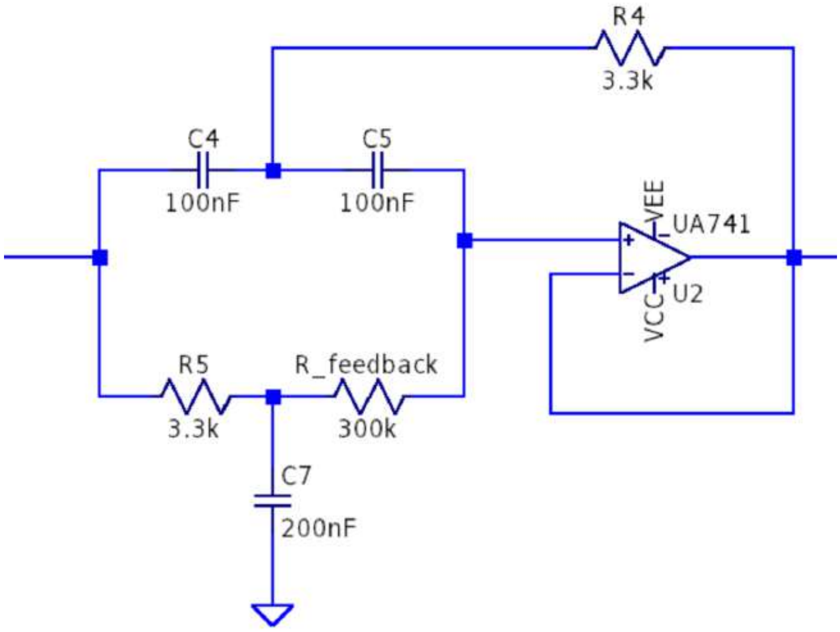

Figure 12: LTSpice Circuit

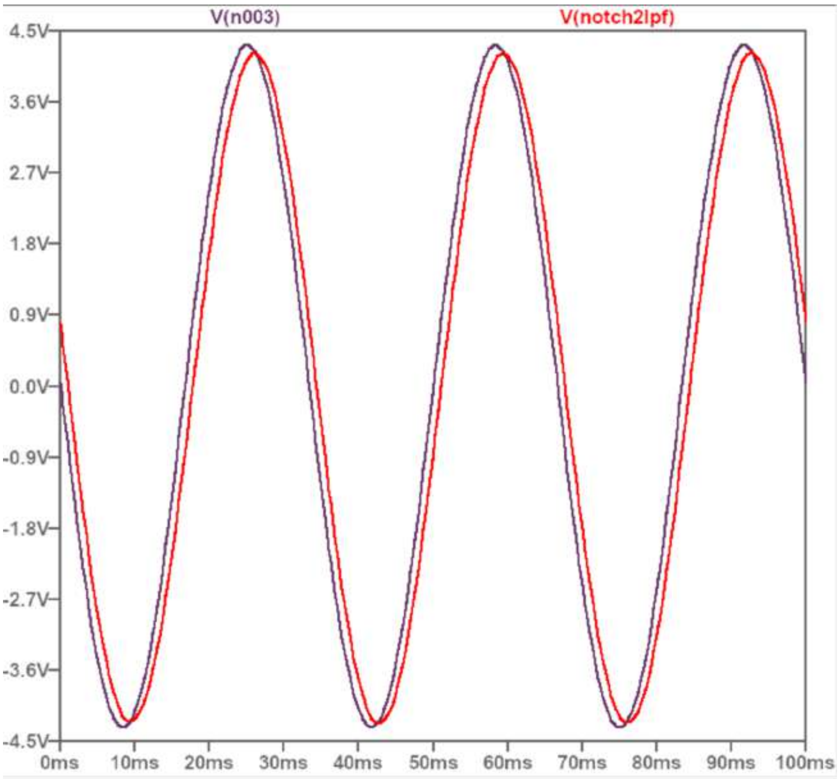

Figure 13: Simulated input output(4.5V sin wave). slight phase shift is observed.

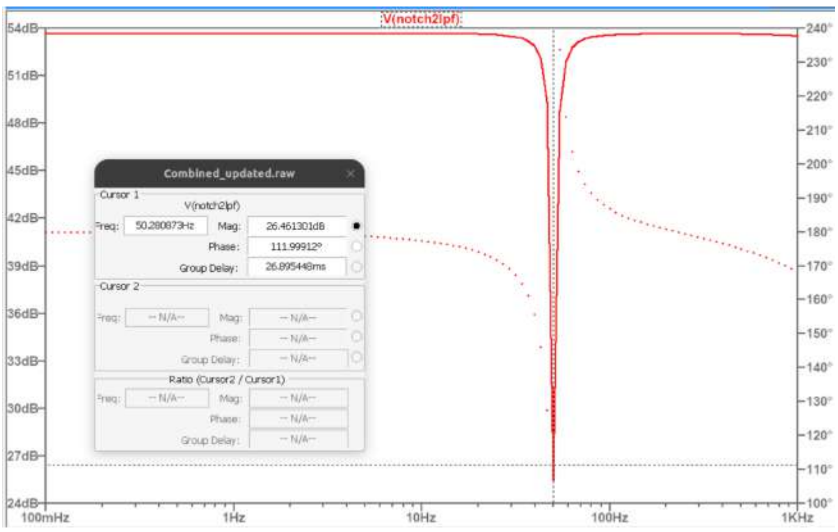

Figure 14: Spice FRA plot, with cursor on cutoff frequency (50Hz). Notice the phase plot sharp change at 50Hz

6.5 Hardware implementation

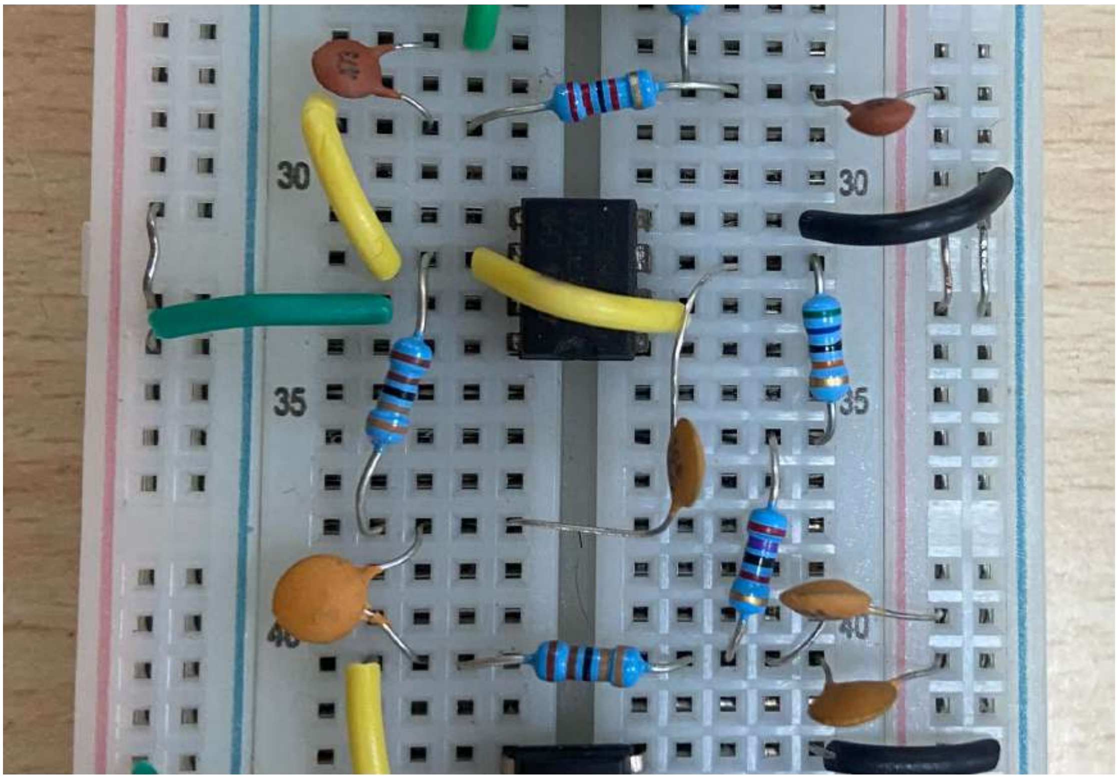

Figure 15: Enter Caption

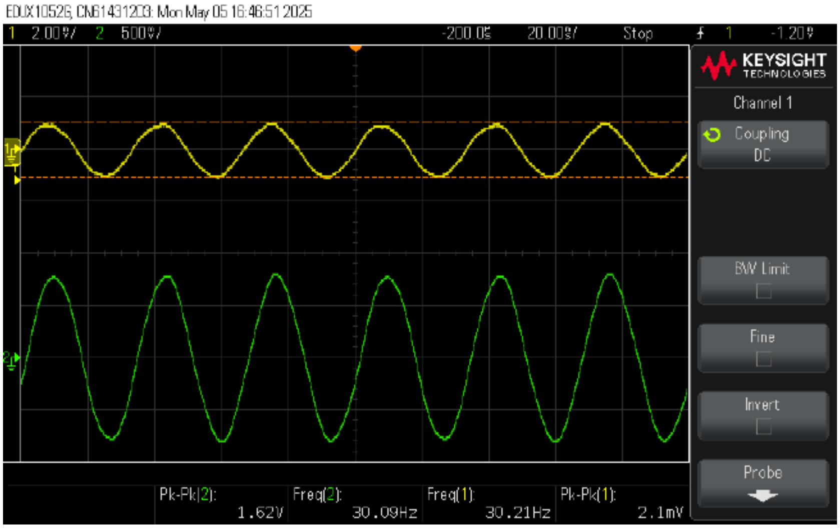

Figure 16: Hardware sim output. previous stage output was 1.72Vpp - gain of 0.9451

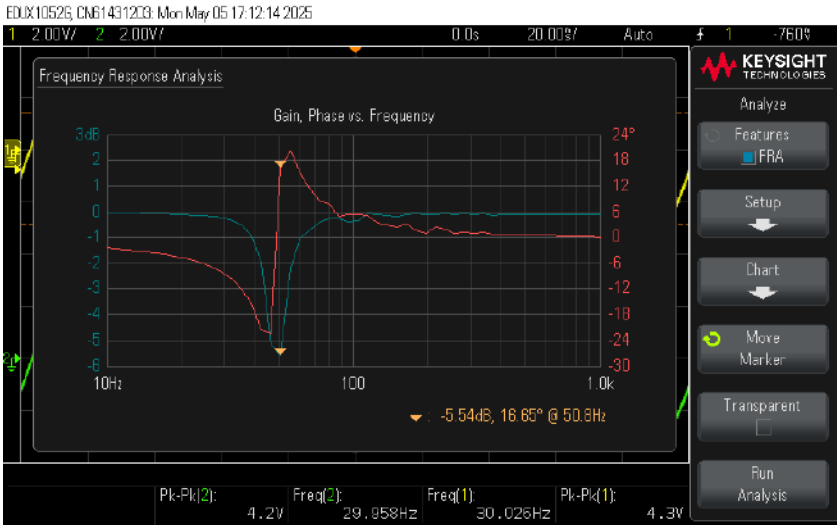

Figure 17: FRA of hardware implentation

6.5.1 Hardware Realization and Challenges

- Realizing this notch filter in hardware was non-trivial due to the sensitivity of the center frequency to resistor and capacitor tolerances.
- Small deviations caused noticeable frequency shifts. This was primarily due to changes in input/output impedance between op-amp and passive branches.

- In hardware, we needed to add an additional resistance of approximately $15\,\Omega$ to match the simulation behavior. This adjustment was determined via trial-and-error.

6.6 Conclusion

The Twin-T notch filter, enhanced with the UA741 op-amp, provides sharp 50 Hz suppression suitable for biomedical signals like ECG. Though simulation gave accurate results, practical implementation required careful tuning due to the sensitivity of the circuit to component variations and impedance mismatches. with a gain of 0.9451.

7 Low-Pass Filter (LPF)

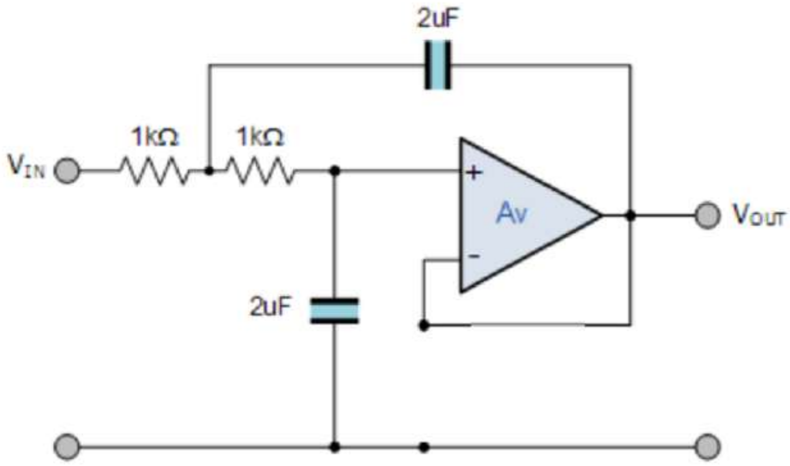

Figure 18: @nd Order LPF circuit, source Electronics stack exchange

7.1 Purpose

A low-pass filter (LPF) is used to suppress high-frequency noise like muscle artifacts (EMG) and electromagnetic interference (EMI), preserving the ECG signal in the typical range of 0.5–100 Hz.

7.2 Theory

A basic passive LPF has a resistor R in series and a capacitor C to ground. Its Laplace-domain transfer function is:

$$H_{\text{LP}}(s) = \frac{1}{sCR + 1}$$

Substituting $s = j\omega$, we get:

$$|H_{\text{LP}}(j\omega)| = \frac{1}{\sqrt{1 + (\omega RC)^2}}$$

The cutoff frequency is:

$$\omega_c = \frac{1}{RC}, \qquad f_c = \frac{1}{2\pi RC}$$

For $R = 22\text{k}\Omega = 22 \times 10^3\ \Omega$, $C = 47\text{nF} = 47 \times 10^{-9}$ F:

$$RC = 22 \times 10^3 \times 47 \times 10^{-9} = 1.034 \times 10^{-3}\ \text{s}$$
$$f_c = \frac{1}{2\pi \cdot RC} = \frac{1}{2\pi \cdot 1.034 \times 10^{-3}} \approx 154\ \text{Hz}$$

The phase response is:

$$\angle H_{\text{LP}}(j\omega) = -\tan^{-1}(\omega RC)$$

7.3 First- vs. Second-Order LPF

A second-order LPF (e.g., Sallen-Key configuration) has a sharper roll-off of 40 dB/decade and can provide improved attenuation of high-frequency components. It uses two resistors and two capacitors along with an op-amp. The transfer function is:

$$H(s) = \frac{1}{1 + \frac{s}{\omega_0 Q} + \left(\frac{s}{\omega_0}\right)^2}$$

where:

$$\omega_0 = \frac{1}{\sqrt{R_1 R_2 C_1 C_2}}, \qquad Q = \frac{\sqrt{R_1 R_2 C_1 C_2}}{R_1 C_1 + R_2 C_1 + R_2 C_2}$$

using: $R_1 = R_2 = 22\text{k}\Omega$, $C_1 = C_2 = 47\text{nF}$, available in Lab

$$\omega_0 = \frac{1}{\sqrt{(22 \times 10^3)^2 \cdot (47 \times 10^{-9})^2}} = \frac{1}{22 \times 10^3 \cdot 47 \times 10^{-9}} \approx 968\ \text{rad/s}$$
$$f_0 = \frac{\omega_0}{2\pi} \approx \frac{968}{2\pi} \approx 154\ \text{Hz}$$
$$Q = \frac{\sqrt{R_1 R_2 C_1 C_2}}{R_1 C_1 + R_2 C_1 + R_2 C_2} = \frac{RC}{RC + RC + RC} = \frac{1}{3} \approx 0.333$$

7.4 Simulation

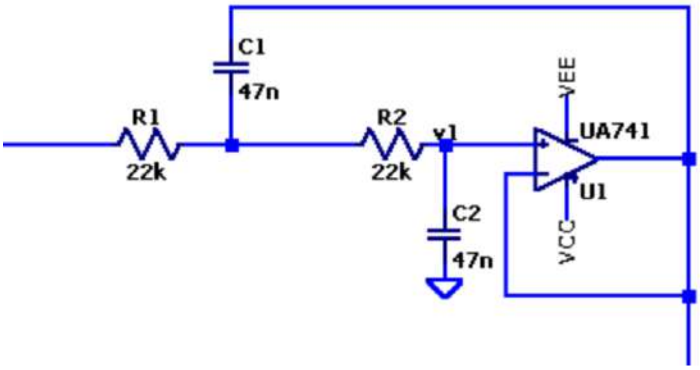

Figure 19: LPF LTspice circuit

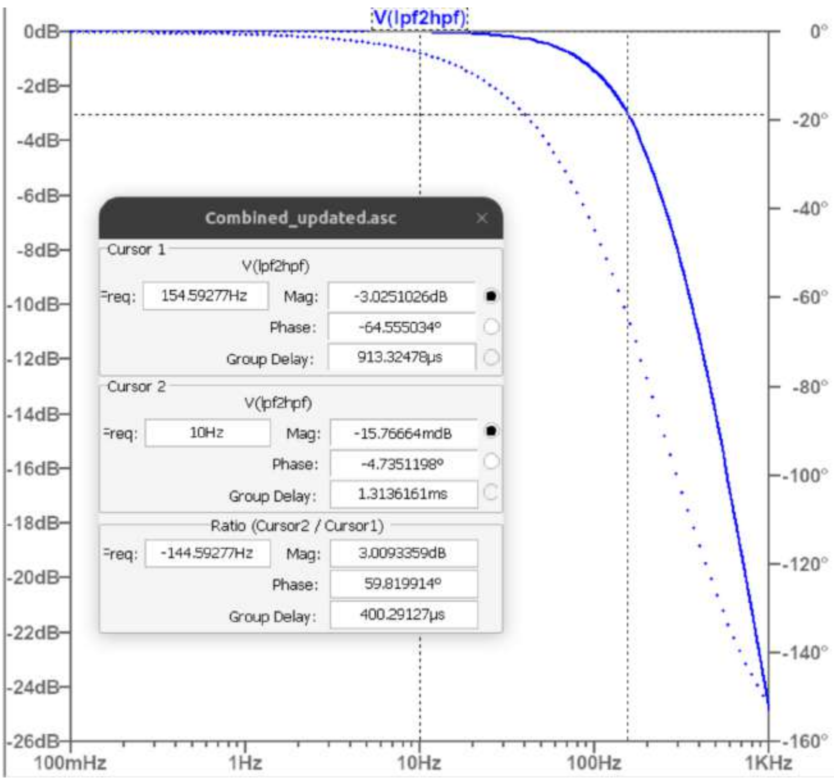

Figure 20: LPF simulation output, cutoff 154Hz

7.5 Hardware Implementation

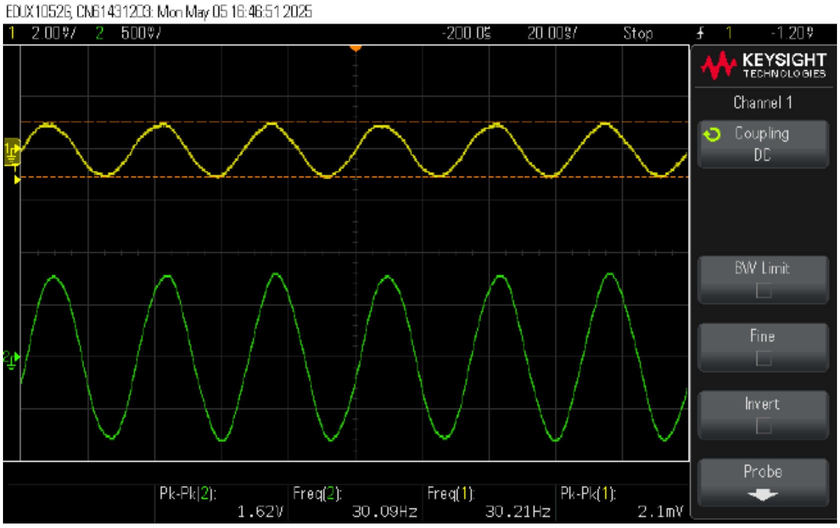

Figure 21: Output to a sinousoidal signal, almost save voltage (0.01V) diffrence between input and output stage. (yellow shows input to Instrumentation amp, please ignore

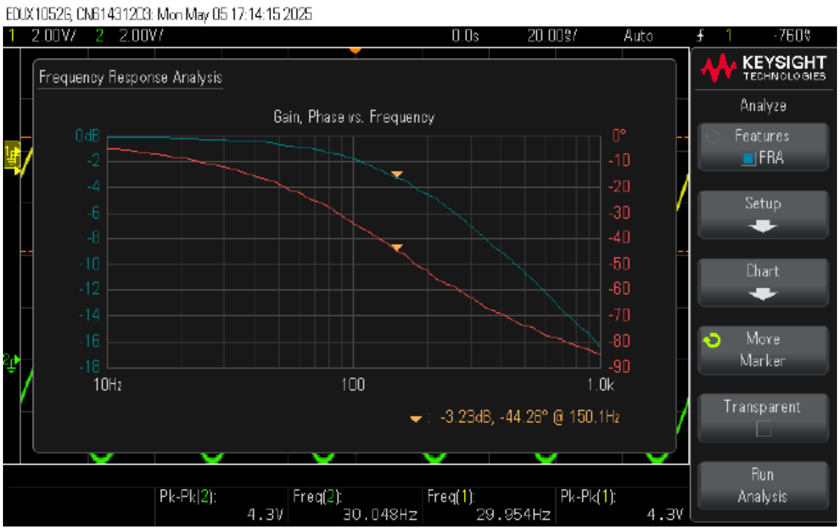

Figure 22: FRA showing cutoff at 150Hz

7.6 Conclusion

The LPF ensures high-frequency noise does not distort the ECG signal. Second-order filters offer better suppression at higher frequencies. With the given component values, a cutoff frequency of approximately 154 Hz is achieved. The second-order configuration further provides a quality factor of about 0.333, offering smoother and sharper attenuation beyond the cutoff. Due to errors, the actual cutoff frequency in hardware was 150Hz, which is within acceptable margin of error.

8 High-Pass Filter (HPF)

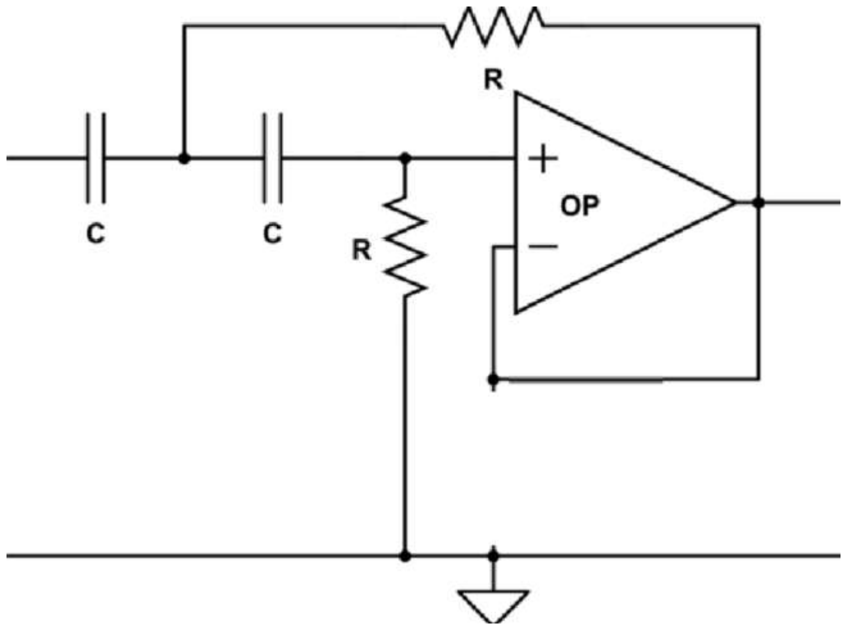

Figure 23: 2nd order HPF circuit. Source eeeguide.com

8.1 Purpose

A high-pass filter (HPF) is used to suppress low-frequency noise and baseline wander (such as breathing artifacts or DC offsets) while preserving the useful ECG signal above the typical threshold of 0.5–1 Hz.

8.2 Theory

A basic passive HPF consists of a capacitor C in series followed by a resistor R to ground. Its Laplace-domain transfer function is:

$$H_{\mathrm{HP}}(s) = \frac{sRC}{1 + sRC}$$

Substituting $s = j\omega$, the magnitude response becomes:

$$|H_{\mathrm{HP}}(j\omega)| = \frac{\omega RC}{\sqrt{1 + (\omega RC)^2}}$$

The cutoff frequency is given by:

$$\omega_c = \frac{1}{RC}, \qquad f_c = \frac{1}{2\pi RC}$$

For $R = 20\,\text{k}\Omega = 10 \times 10^3\ \Omega$, $C = 100\,\mu\text{F} = 100 \times 10^{-6}$ F:

$$RC = 20 \times 10^3 \times 100 \times 10^{-6} = 2 \text{ s}$$

$$f_c = \frac{1}{2\pi \cdot RC} = \frac{1}{2\pi \cdot 2} \approx 0.785 \text{ Hz}$$

To get a sharper roll-off, a second-order HPF is used. The Sallen-Key configuration with two capacitors and two resistors has the following transfer function:

$$H(s) = \frac{s^2}{s^2 + \frac{\omega_0}{Q}s + \omega_0^2}$$

where:

$$\omega_0 = \frac{1}{\sqrt{R_1R_2C_1C_2}}, \qquad Q = \frac{\sqrt{R_1R_2C_1C_2}}{R_1C_2 + R_1C_1 + R_2C_2}$$

Using: $R_1 = R_2 = 20\,\text{k}\Omega$, $C_1 = 10\,\mu\text{F}$, $C_2 = 100\,\mu\text{F}$:

$$\begin{aligned}
RC &= 20 \times 10^3 \times 10 \times 10^{-6} = 0.2 \text{ s} \\
\omega_0 &= \frac{1}{\sqrt{(20 \times 10^3)^2 \cdot 10 \times 10^{-6} \cdot 100 \times 10^{-6}}} = \frac{1}{\sqrt{4 \times 10^8 \cdot 10^{-3}}} \\
&= \frac{1}{\sqrt{4 \times 10^5}} = \frac{1}{632.46} \approx 1.58 \text{ rad/s} \\
f_0 &= \frac{\omega_0}{2\pi} \approx \frac{1.58}{2\pi} \approx 0.251 \text{ Hz} \\
Q &= \frac{632.46}{20 \times 10^3 \cdot (100 + 10 + 100) \times 10^{-6}} = \frac{632.46}{20 \times 10^3 \cdot 210 \times 10^{-6}} \\
&= \frac{632.46}{4.2} \approx 0.15
\end{aligned}$$

8.3 Simulation

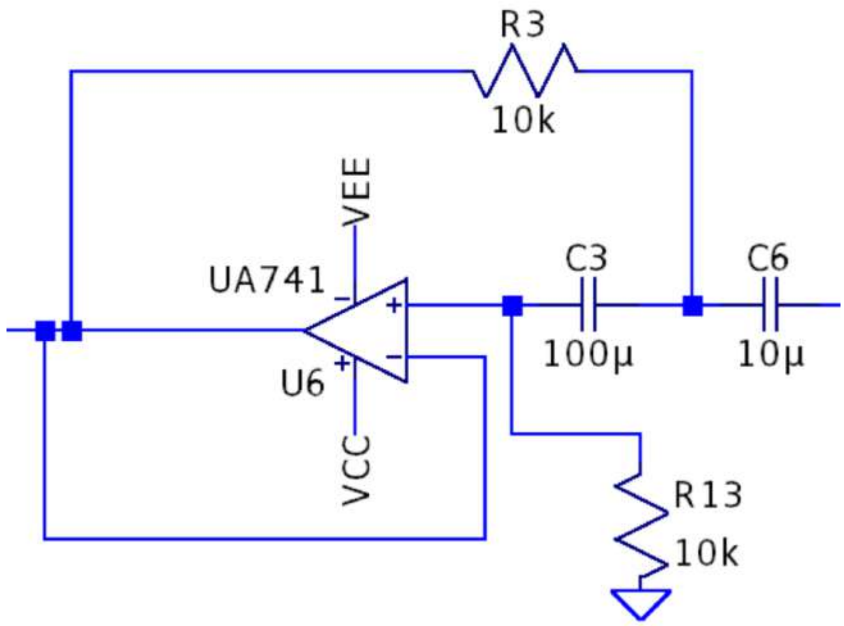

Figure 24: HPF circuit. Please note it's in reverse direction from reference diagram

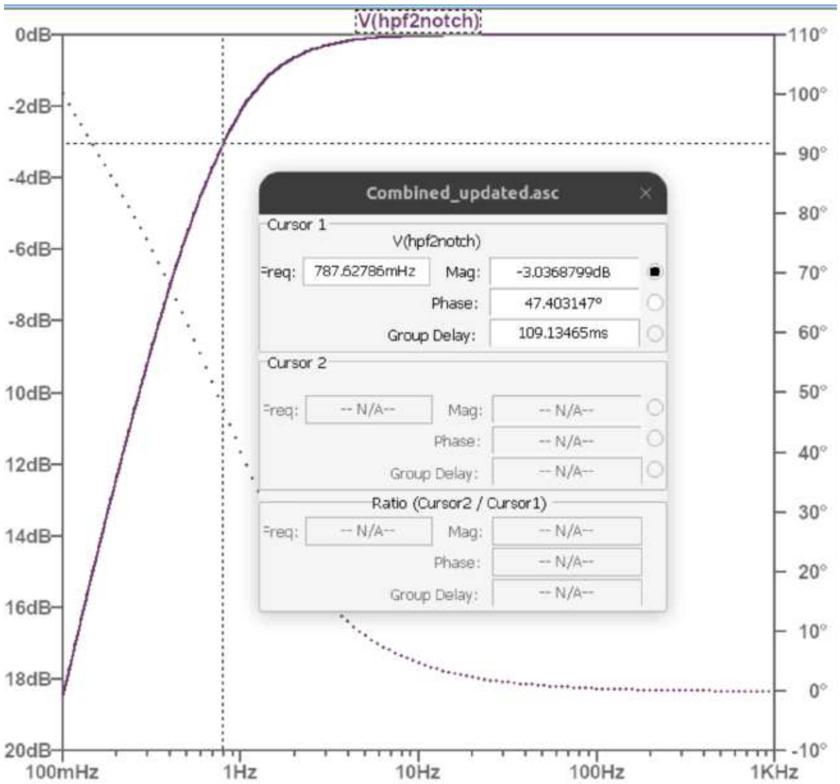

Figure 25: HPF simulation BODE plot.

8.4 Hardware Implementation

The DSO doesnt support such low frequencies we are dealing with. So we had to manually supply frequency using wavegen and compare.

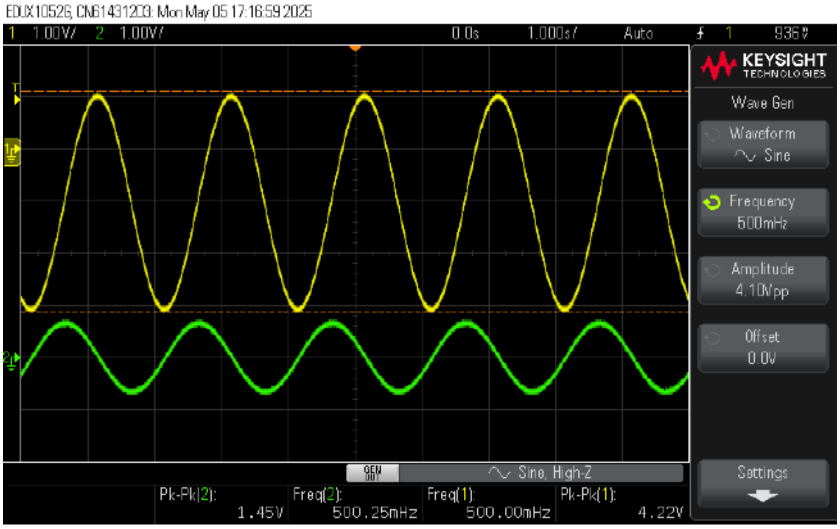

Figure 26: attenuating to 1.45V for 4.2V input at 500mHz

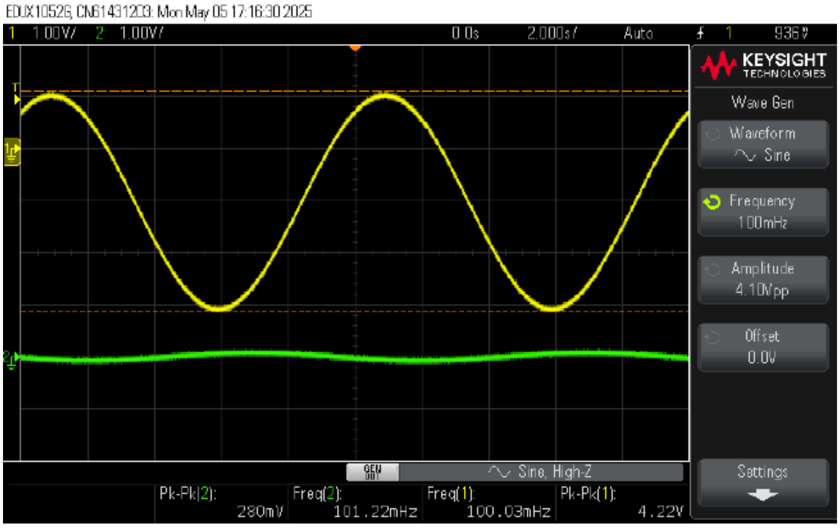

Figure 27: attenuating to 280mV for 4.2V input at 100mHz

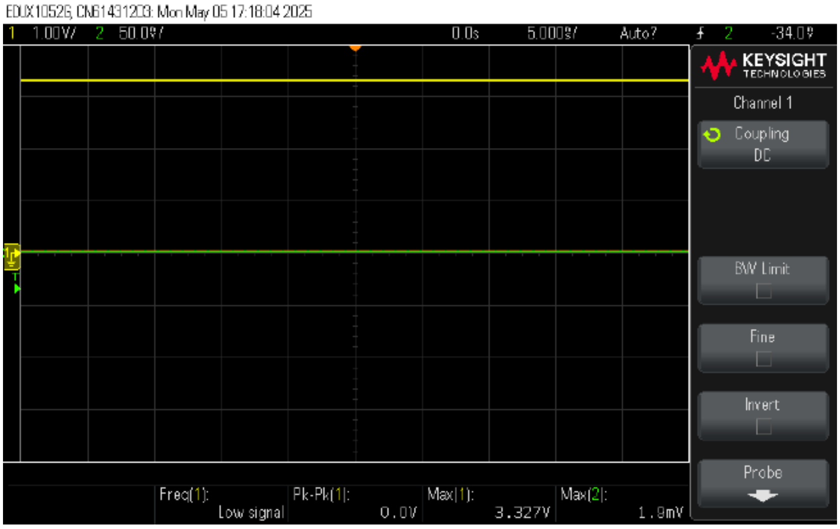

Figure 28: 1.9mV output for a DC input of 3.3V (blocking 0 Hz frequency)

8.5 Conclusion

The HPF is effective in eliminating baseline drift and very low-frequency components such as those introduced by patient movement or respiration. The actual hardware implementation closely matches the simulation, with a measured cutoff of approximately 0.47–0.5 Hz using available lab components. Slight variations are acceptable due to capacitor tolerances and input impedance mismatches.

9 Final Integration

9.1 Simulated plots

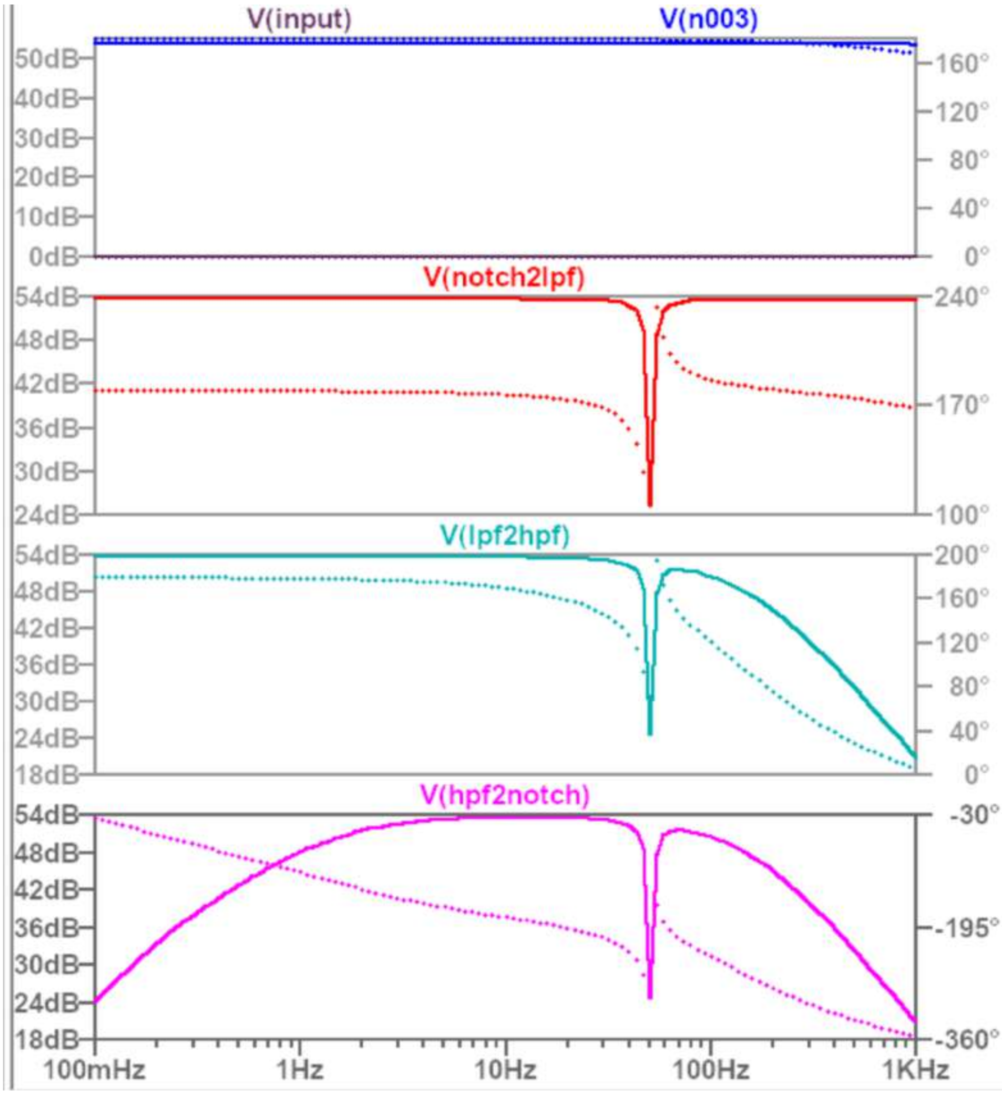

Figure 29: Plots of FRA of various stages

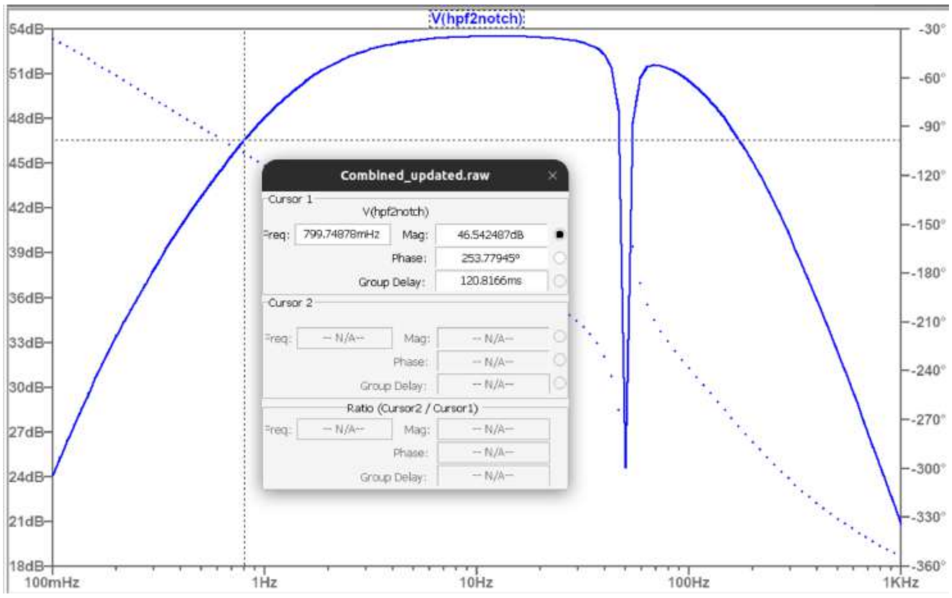

Figure 30: Final FRA plot, showing bandpass behaviour and notch filtering

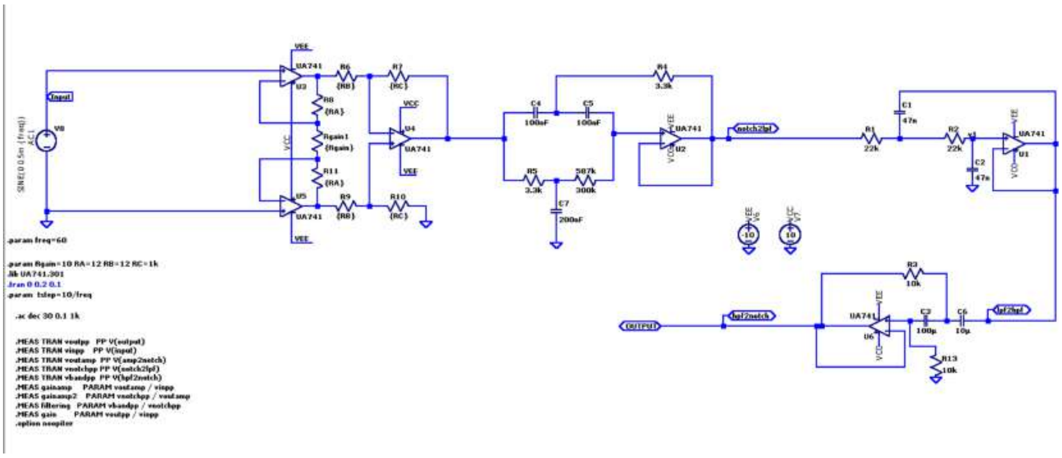

Figure 31: Full circuit in Spice

9.2 Hardware plots

Figure 32: Plot showing notch at 49.8Hz

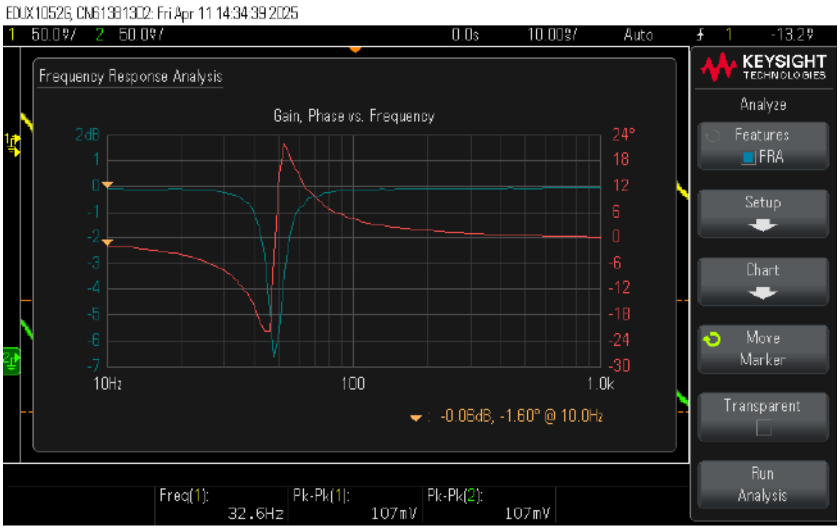

Figure 33: FRA plot of notch filter, howing proper notch

Table 1: Summary of Theoretical, Simulated, and Hardware Results for Each Filter Stage

Filter Stage	Theoretical Output	Simulated Output	Hardware Output
Notch Filter (50 Hz)	Notch at 50 Hz, $Q \approx 9.09$, $f_0 \approx 49.7$ Hz	Deep notch at 50 Hz, phase shift observed	Notch near 50 Hz, Gain ≈ 0.9451, slight frequency shift due to tolerances
Low-Pass Filter	Cutoff $f_c \approx 154$ Hz, 2nd order, $Q \approx 0.333$	Cutoff at 154 Hz, clean roll-off	Cutoff at $\sim$150 Hz, minor voltage drop (0.01V), matches simulation
High-Pass Filter	Cutoff $f_c \approx 0.08$ Hz ($R = 20\text{k}\Omega$, $C = 100\mu\text{F}$)	Passes signal above 0.1 Hz, attenuates DC component	Cutoff near 0.5 Hz, removes baseline wander due to breathing, slight phase shift

10 Testing on Humans

Now, the completed circuit was ready to be tested on humans. The circuit was tested on a 5'7", 65Kg, 21Y old Male. the plots obtained were good enough to detect heart rate, and usable for ADC based processing for removing more noise.

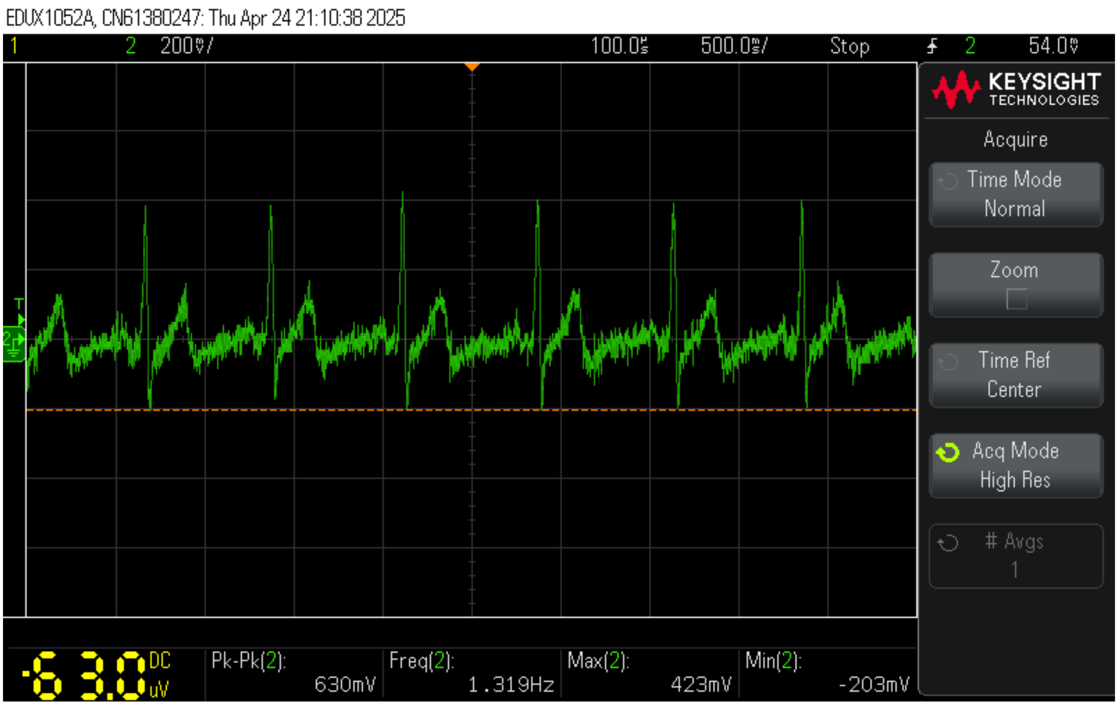

Figure 34: ECG output showing PQRT waves

- ECG waveforms (P, QRS, T) were observable on oscilloscope.
- Noise was significantly reduced using HPF, LPF, and notch filter.
- Common-mode rejection was crucial for clarity.
- Proper electrode placement and contact resistance affected signal quality.

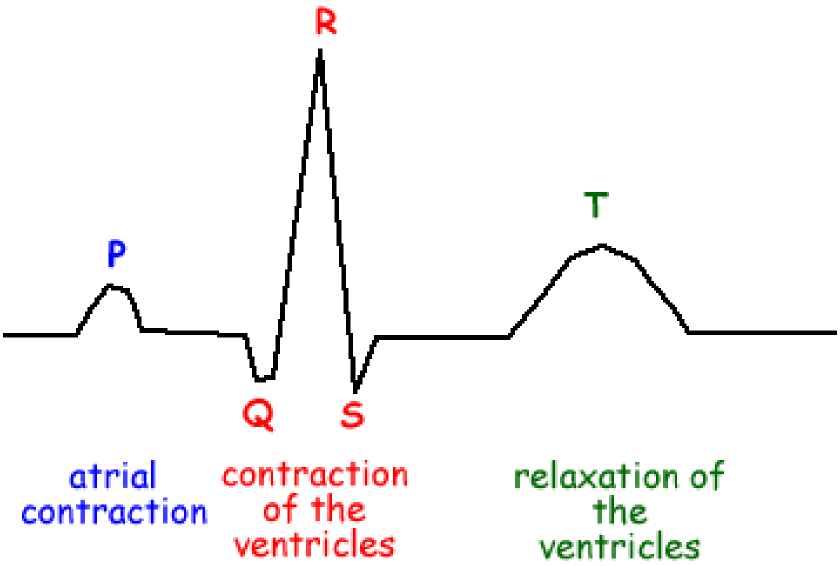

Figure 35: P-QRS-T plot of ECG

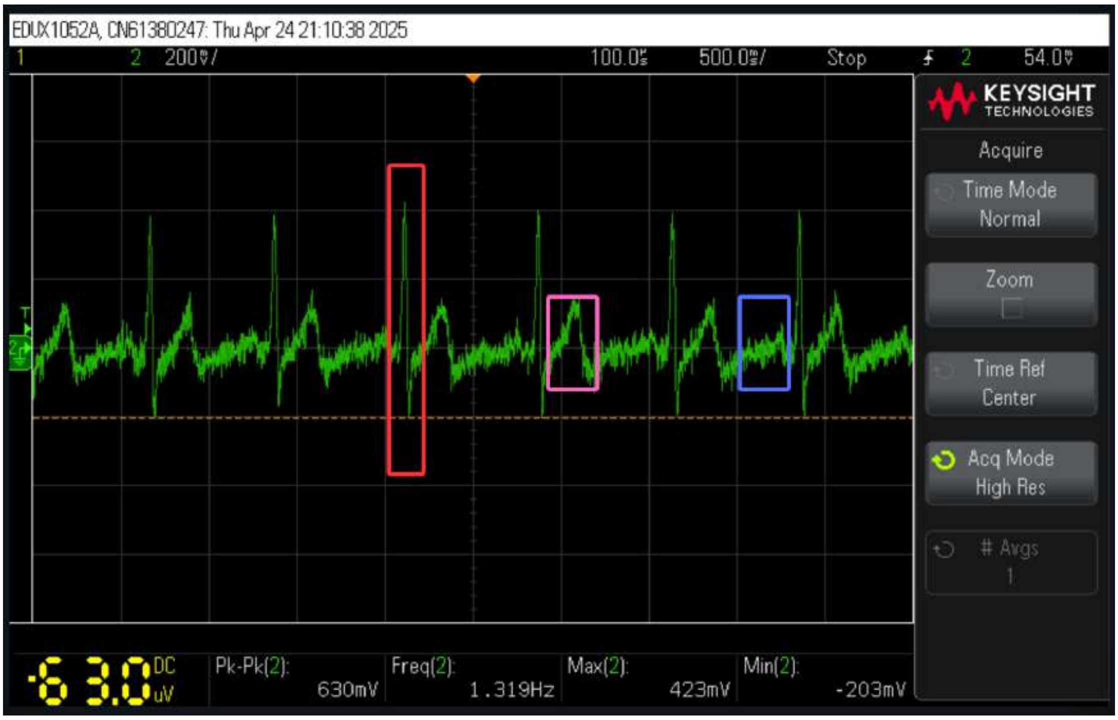

Figure 36: P - Purple, QRS - Red , T - pink, these charecteristics are more clear after processing as can be seen later

10.1 Output Verification

The output of the ECG circuit can be verified using several key methods to ensure its accuracy and reliability. The following aspects were considered during the verification process:

- **Heartbeat Accuracy:** The first verification step involved comparing the output of the ECG signal to the actual heartbeat. The recorded heartbeat was consistently within a 2-3 beats per minute (BPM) range of my real heartbeat, as measured by the Fitbit Versa 2, ensuring the accuracy of the ECG signal.

- **Pulse Characteristics:** Another critical aspect of verification was ensuring that all pulse characteristics of the ECG waveform, including the P-wave, QRS complex, and T-wave, were clearly visible in the output. The signal displayed the expected characteristics, confirming that the circuit was functioning as intended.

- **Common Mode Noise Rejection:** Common mode noise rejection was another important factor to assess. This was already verified through the use of the instrumentation amplifier, which demonstrated effective noise rejection. No significant interference was observed in the output ECG signal.

All these verification steps were performed successfully, confirming that the ECG circuit produces accurate and reliable results suitable for further analysis or use as a pre-stage to an ADC for digital ECG processing.

11 ECG Signal Acquisition and Processing

The ECG signal was recorded using a digital oscilloscope (DSO) and exported as a CSV file containing time and voltage data. After estimating the sampling frequency, very high-order digital filters were applied: a bandpass filter (0.5 Hz to 100 Hz) to isolate the heart signal and a notch filter at 50 Hz to remove powerline noise. These filters helped clean the signal significantly. Adaptive peak detection was then used to identify heartbeats by dynamically adjusting the threshold based on the filtered signal's characteristics. The estimated heart rate from this process closely matched my Fitbit reading at that moment, validating the approach. With the signal now clean and key features extracted, it can be further processed for advanced ECG analysis like QRS complex identification, arrhythmia detection, or heart rate variability, using straightforward digital methods.

This clearly demonstrated the capability of our circuit to be used as input to an ADC for further digital processing and actual medicinal use.

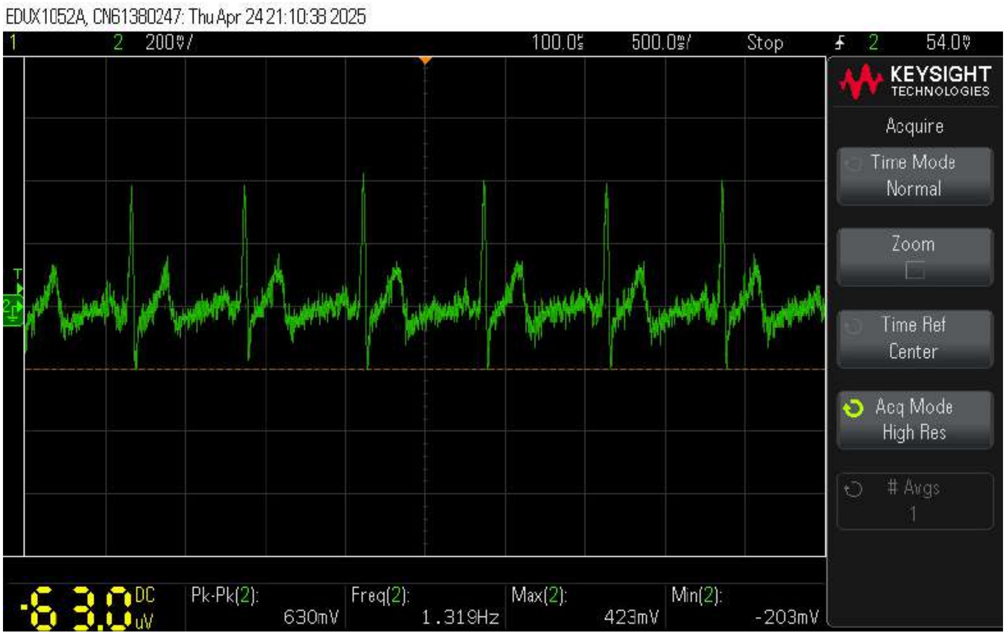

Figure 37: Raw ECG signal as captured from the DSO on the CSV file

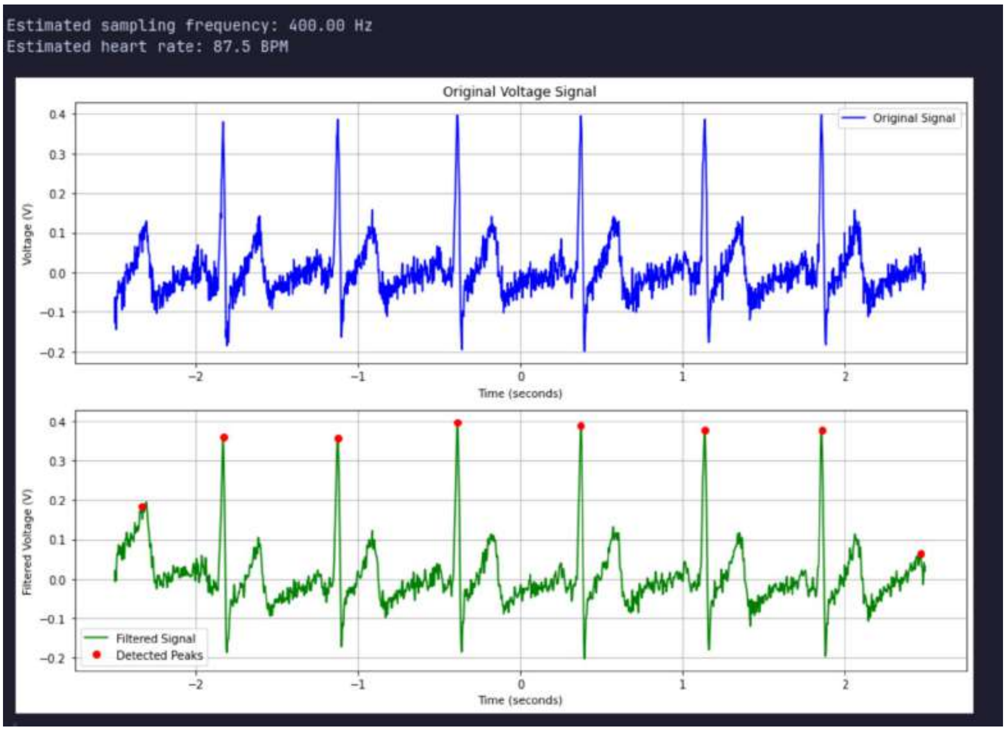

Figure 38: Filtered ECG signal after Signal Processing, giving a reading of 87.5 bpm (beats per minute)

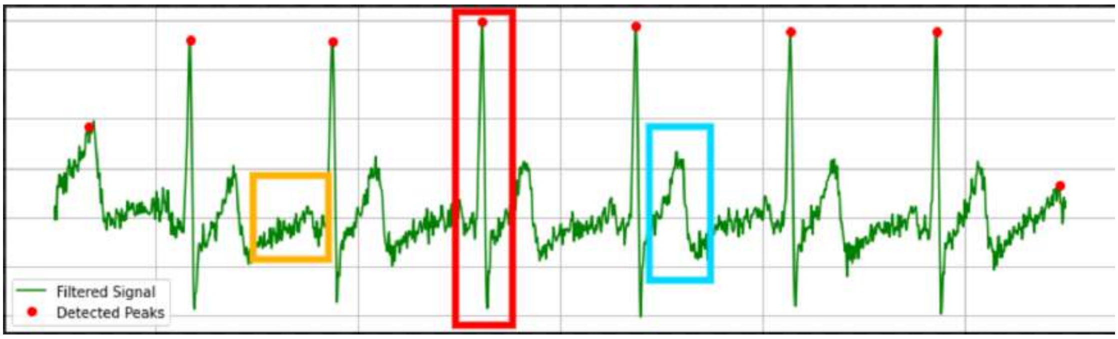

Figure 39: P - Orange, QRS - Red , T - Blue, clearly visible in this processed CSV acquired from our circuit.

12 Video Demonstration

Demonstration of how the entire circuit works in unison, please refer to the following video:

Complete ECG Circuit Working Video

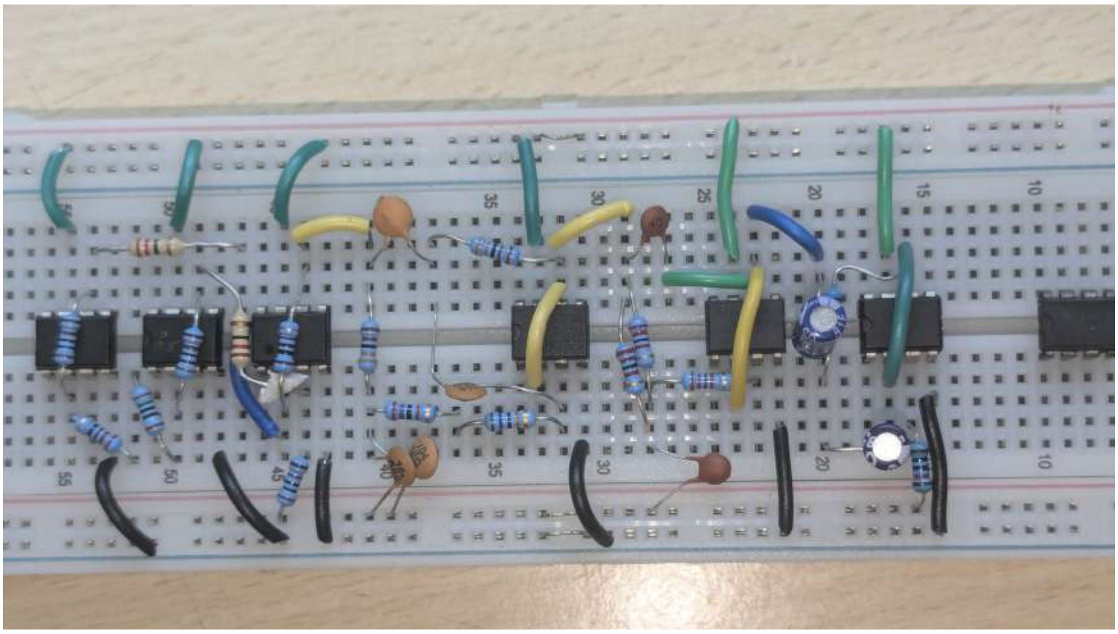

Figure 40: Complete Circuit Image

13 Conclusion

The ECG signal acquisition and processing circuit developed in this project demonstrated the capability to extract meaningful cardiac signals using an analog front-end composed of amplification, filtering, and noise reduction stages. The results show that even with basic components and careful design, one can retrieve a relatively clean ECG waveform suitable for analysis. The performance was validated across theoretical, simulated, and hardware stages, proving the effectiveness of the design approach.

13.1 Low-Cost and ADC Integration Potential

This low-cost ECG device is not only affordable and easy to build but also functions effectively as a preliminary stage for further digitization. Its signal conditioning capabilities make it an excellent candidate for feeding into an ADC (Analog-to-Digital Converter), paving the way for integration with digital ECG processing systems, mobile health monitors, or embedded systems. Given its simplicity and affordability, the circuit can serve as an educational tool or even a prototype in wearable health tech development.

13.2 Challenges and Observations

Several practical challenges were encountered throughout the project. Signal acquisition was particularly sensitive to noise, requiring careful probe placement and shielding. Muscle artifacts and environmental interference (especially 50/60 Hz mains noise) posed filtering challenges. While bandpass filtering helped, fine-tuning the cutoff frequencies without distorting the QRS complex proved tricky. In addition, variability in skin-electrode contact and the use of makeshift probes often led to inconsistent signal amplitudes and occasional baseline wandering, which was later fixed using a high pass filter. These issues highlight the importance of both robust hardware and algorithmic post-processing in practical biomedical systems.

13.3 Acknowledgements

We would like to sincerely thank our course instructor Prof Spandan, Prof Arti & Prof Madhav , teaching assistants (especially our alloted TA, Mallika Garg) and Lab assitants, Gopal Rao Sir and Prashant Sir for their guidance, timely feedback, and support throughout the project. Their insights were critical in helping us troubleshoot circuit issues, understand the underlying physiology, and push the project toward a successful outcome.

References

[1] Electronics Tutorials. "Butterworth Filter Design - Basic Electronics Tutorials and Revision." Electronics Tutorials, n.d. Available: https://www.electronics-tutorials.ws/filter/filter_8.html. Accessed: May 5, 2025.

[2] All About Circuits. "An Introduction to Filters - Technical Articles." All About Circuits, n.d. Available: https://www.allaboutcircuits.com/technical-articles/an-introduction-to-filters/. Accessed: May 5, 2025.

[3] Texas Instruments. "Instrumentation Amplifiers — TI.com." Texas Instruments, n.d. Available: https://www.ti.com/amplifier-circuit/instrumentation/overview.html. Accessed: May 5, 2025.

[4] BIOPAC Systems. "ECG Guide." BIOPAC Systems, n.d. Available: https://www.biopac.com/wp-content/uploads/ECG-Guide.pdf. Accessed: May 5, 2025.

[5] Mindray. "Mindray ECG Lead Placement Quick Reference Guide." Mindray, n.d. Available: https://www.mindray.com/content/dam/xpace/en_us/service-and-support/training-and-education/resource--library/modality/quick-reference-guides-1/Mindray-ECG-Lead-Placement_7664B.pdf. Accessed: May 5, 2025.

13.4 Code used for signal processing the CSV file

```
import numpy as np
import matplotlib.pyplot as plt
from scipy import signal
from scipy.signal import find_peaks
import os


file_path = "scope_60.csv"

try:

    with open(file_path, "r") as file:
        lines = file.readlines()


    data_lines = lines[2:]


    time_values = []
    voltage_values = []

    for line in data_lines:
        line = line.strip()
        if line:
            time_str, voltage_str = line.split(",")
            time_values.append(float(time_str))
            voltage_values.append(float(voltage_str))
```

```
    time = np.array(time_values)
    voltage = np.array(voltage_values)


    if len(time) > 1:

        dt = np.mean(np.diff(time))
        fs = 1 / abs(dt)
    else:
        fs = 1

    print(f"Estimated sampling frequency: {fs:.2f} Hz")



    order = 3
    lowcut = 0.5  # Hz
    highcut = 100  # Hz

    def butter_bandpass(lowcut, highcut, fs, order=5):
        nyq = 0.5 * fs
        low = lowcut / nyq
        high = highcut / nyq
        b, a = signal.butter(order, [low, high], btype="band")
        return b, a

    def butter_bandstop(lowcut, highcut, fs, order=10):
        nyq = 0.5 * fs
        low = lowcut / nyq
        high = highcut / nyq
        b, a = signal.butter(order, [low, high], btype="bandstop")
        return b, a

    def butter_bandpass_filter(data, lowcut, highcut, fs, order=5):
        b, a = butter_bandpass(lowcut, highcut, fs, order=order)
        y = signal.filtfilt(b, a, data)
        return y
```

```python

def butter_bandstop_filter(data, lowcut, highcut, fs, order=10):
    b, a = butter_bandstop(lowcut, highcut, fs, order=order)
    y = signal.filtfilt(b, a, data)
    return y

def combined_filter(data, bp_lowcut, bp_highcut, bs_lowcut, bs_highcut, fs, bp_order=5, bs_order=5):
    bandpassed = butter_bandpass_filter(data, bp_lowcut, bp_highcut, fs, bp_order)
    filtered = butter_bandstop_filter(bandpassed, bs_lowcut, bs_highcut, fs, bs_order)

    return filtered


filtered_voltage = combined_filter(voltage, lowcut, highcut , 49 , 51 , fs, order , 5 )



distance = int(fs * 0.5)
peaks, _ = find_peaks(filtered_voltage, distance=distance)


if len(peaks) > 1:

    peak_times = time[peaks]
    intervals = np.diff(peak_times)
    mean_interval = np.mean(intervals)


    heart_rate = 60 / mean_interval
    print(f"Estimated heart rate: {heart_rate:.1f} BPM")


plt.figure(figsize=(12, 8))


plt.subplot(2, 1, 1)
```

```python
    plt.plot(time, voltage, "b-", label="Original Signal")
    plt.grid(True)
    plt.xlabel("Time (seconds)")
    plt.ylabel("Voltage (V)")
    plt.title("Original Voltage Signal")
    plt.legend()


    plt.subplot(2, 1, 2)
    plt.plot(time, filtered_voltage, "g-", label="Filtered
       Signal")
    plt.plot(time[peaks], filtered_voltage[peaks], "ro",
       label="Detected Peaks")


    plt.grid(True)
    plt.xlabel("Time (seconds)")
    plt.ylabel("Filtered Voltage (V)")
    plt.legend()

    plt.tight_layout()
    plt.show()

except Exception as e:
    print(f"err {e}")
```